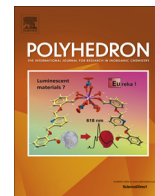




Contents lists available at ScienceDirect

Polyhedron

journal homepage: www.elsevier.com/locate/poly

Iridium complexes containing N-donor-functionalized η^1 -fluorenyl ligands

Fioralba Taullaj^a, David Armstrong^a, Alan J. Lough^b, Ulrich Fekl^{a,*}

^a Department of Chemical and Physical Sciences, University of Toronto Mississauga, 3359 Mississauga Road, Mississauga, ON L5L 1C6, Canada

^b X-ray Crystallography Lab, University of Toronto St. George, 80 St. George St., Toronto, ON M5S 3H6, Canada

ARTICLE INFO

Article history:

Received 2 June 2015

Accepted 24 August 2015

Available online xxxxx

Keywords:

Constrained geometry

Fluorenyl

Nitrogen donor

Late metal

Hydrogenation

ABSTRACT

Iridium complexes of two different nitrogen-donor-functionalized fluorenyl ligands have been synthesized and characterized, $L^1Ir(COD)$ and $L^2Ir(COD)$, where $L^{1-} = [9-(2\text{-dimethylamino)ethyl}]fluorenyl$ anion, $L^{2-} = [9-(2\text{-ortho-pyridyl)ethyl}]fluorenyl$ anion, and $COD = 1,5\text{-cyclooctadiene}$. The structures of both ligands (in their protonated form) and of both complexes were determined by single-crystal X-ray crystallography. Structural consequences of the nature of the nitrogen ligand (dimethylamino substituent versus *ortho*-pyridyl substituent) are significantly different Ir–N distances (shorter for $L^2Ir(COD)$) and indirect *cis*-influence on the COD ligand resulting in a shorter Ir–olefin bond *cis* to the nitrogen donor in $L^2Ir(COD)$. Both complexes act as precatalysts for arene hydrogenation.

© 2015 Elsevier Ltd. All rights reserved.

1. Introduction

Constrained geometry complexes are an important class of compounds [1]. They typically involve a π -donor (cyclopentadienyl or substituted cyclopentadienyl) ligand tethered with a short linker (bridge) to a group containing a donor atom (Fig. 1).

Most often used for olefin polymerization, these complexes became popular in part due to their increased thermal stability over traditional metallocene catalysts [2]. Other transformations that can be catalyzed by constrained geometry complexes include polar bond hydrogenation as well as hydroboration, hydroamination, and hydrosilylation of olefins [3].

The majority of constrained geometry complexes contain early transition metals or rare-earth metals [3]. There are very few examples of constrained geometry complexes of late transition metals [4]. Motivated in part by the potential for hydrogenation catalysis, we set out to synthesize constrained geometry complexes of iridium, using the two potentially π -donating ligands L^{1-} , [9-(2-dimethylamino)ethyl]fluorenyl anion, and L^{2-} , [9-(2-*ortho*-pyridyl)ethyl]fluorenyl anion. Specifically, the iridium (I) complexes $L^1Ir(COD)$ and $L^2Ir(COD)$ were obtained ($COD = 1,5\text{-cyclooctadiene}$). Whether the ligands L^{1-} and L^{2-} actually act as constrained geometry π -donating ligands (η^5 -fluorenyl residue) or as σ -donor ligands (with η^1 -bound fluorenyl residue) will depend on many factors. It is known from a related potentially

π -coordinating ligand that the same ligand can switch binding modes, even with the same metal, depending on oxidation state and ligand environment of the metal [4]. As will be detailed below, in $L^1Ir(COD)$ and $L^2Ir(COD)$ both L^{1-} and L^{2-} act as C,N σ -donors (η^1 -fluorenyl) and not as π -donating constrained geometry ligands. Preliminary hydrogenation studies with the two complexes suggest that under mild H_2 pressures (1 atm) and ambient temperature, these complexes are reduced to finely dispersed iridium metal which performs heterogeneous arene hydrogenation under the reaction conditions, such that $L^1Ir(COD)$ and $L^2Ir(COD)$ act as precatalysts for arene hydrogenation.

2. Results and discussion

2.1. Synthesis

The procedure for the synthesis of $L^1Ir(COD)$ is depicted in Scheme 1. This procedure was applied analogously for the synthesis of $L^2Ir(COD)$, where 2-(bromomethyl)pyridine hydrobromide was substituted for 2-chloro-N,N-dimethylethylamine hydrochloride.

The synthetic procedure was designed such as to allow for facile synthesis of both the ligands and final complexes. Various synthetic procedures for both ligands have been reported previously [5], however these procedures employ column chromatography for purification of the final product. It is known that large, organic cations can be cleanly precipitated from aqueous solution using hexafluorophosphate anion [6]. We therefore chose to purify the ligands through the use of a salt metathesis reaction. Addition of

* Corresponding author. Tel.: +1 905 828 3806.

E-mail address: ulrich.fekl@utoronto.ca (U. Fekl).

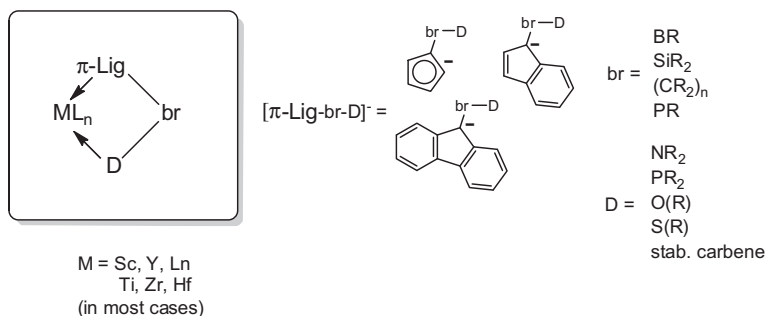
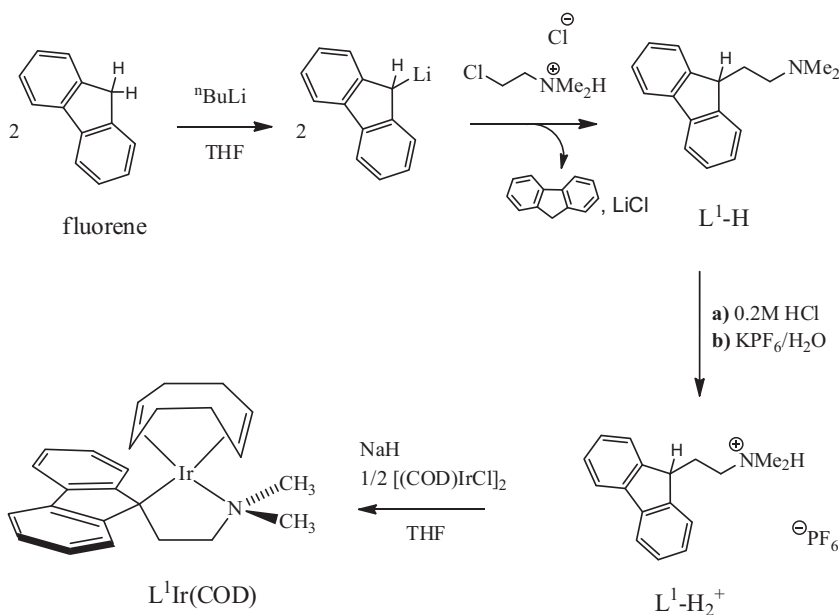


Fig. 1. Variability of constrained geometry complexes.

Scheme 1. Synthetic procedure for $L^1\text{Ir(COD)}$.

KPF_6 to doubly protonated (at C and N) ligands, denoted as $L^1\text{-H}_2^+$ and $L^2\text{-H}_2^+$, soluble in the form of the chloride salts, produced the less soluble and crystalline hexafluorophosphate salts (Scheme 1). For transfer onto iridium, a one-pot synthesis was employed, in which deprotonation of the respective ligand by excess NaH in the presence of $[\text{Ir(COD)Cl}]_2$ led to successful transmetalation onto iridium. Yields for the ligands are fair-to-good and yields for metallation onto iridium are excellent: $L^1\text{-H}_2^+ \text{PF}_6^-$ and $L^1\text{-H}_2^+ \text{PF}_6^-$ were synthesized in 50% yield and 66% yield, respectively. A close to quantitative yield of 95% was obtained for both metallations, to yield $L^1\text{Ir(COD)}$ and $L^2\text{Ir(COD)}$.

2.2. X-ray crystal structures

Crystals suitable for X-ray diffraction were obtained by recrystallization from dichloromethane for both $L^1\text{-H}_2^+ \text{PF}_6^-$ and $L^1\text{-H}_2^+ \text{PF}_6^-$, and by recrystallization from concentrated toluene solutions for $L^1\text{Ir(COD)}$ and $L^2\text{Ir(COD)}$. The structures were solved and refined with standard methods (details in Table 1). Anisotropic displacement plots for the structures of $L^1\text{-H}_2^+$, (nitrogen-protonated $L^1\text{-H}$), $L^2\text{-H}_2^+$, $L^1\text{Ir(COD)}$ and $L^2\text{Ir(COD)}$ are given in Fig. 2.

The structures of $L^1\text{Ir(COD)}$ and $L^2\text{Ir(COD)}$ are closely related. Both $L^1\text{Ir(COD)}$ and $L^2\text{Ir(COD)}$ show pseudo-square planar geometry about the iridium center if the center of each COD π -bond is

counted as a ligand. Both complexes exhibit η^1 -binding of the anionic fluorenyl moiety. Several interesting structural features are observed in the two complexes. First, the Ir–N bond lengths show a significant difference between the two complexes. The Ir–N distance in $L^1\text{Ir(COD)}$ is 2.180 Å whereas the corresponding Ir–N distance in $L^2\text{Ir(COD)}$ is 2.099 Å. The effect observed is in accord with literature findings: a search of the CSD reveals that the average Ir–N distance for iridium coordinated to sp^3 nitrogen donors (788 examples) is 2.146 Å, while the average Ir–N distance for sp^2 nitrogen donors (8293 examples) is shorter, 2.089 Å (see Supporting information). This is in part, of course, an electronic effect, since the donor orbital for a pyridyl donor (ca. sp^2) has more s-character and is thus more compact than the donor orbital for an amine donor (ca. sp^3). A pronounced and unexpected difference between the two complexes concerns the iridium–olefin bond lengths, and this appears to be due to a steric effect. The iridium–olefin bond length *trans* to the nitrogen donor is almost the same for both complexes, at 2.026 Å for $L^1\text{Ir(COD)}$ and 2.028 Å for $L^2\text{Ir(COD)}$. In contrast the iridium–olefin distance *trans* to the fluorenyl carbanion, that is *cis* to the nitrogen donor, shows a drastic difference with a distance of 2.128 Å for $L^1\text{Ir(COD)}$ and 2.016 Å for $L^2\text{Ir(COD)}$. Since the ligand *trans* is the same in both cases (alkyl-substituted fluorenyl), this is almost certainly the result of a *cis* influence. The increased Ir–olefin bond length for $L^1\text{Ir(COD)}$

Table 1
Crystal and Structure refinement for $L^1-H_2^+ PF_6^-$ and $L^2-H_2^+ PF_6^-$, $L^1Ir(COD)$, $L^2Ir(COD)$.

	$L^1-H_2^+ PF_6^-$	$L^2-H_2^+ PF_6^-$	$L^1Ir(COD)$	$L^2Ir(COD)$
Empirical formula	$C_{17}H_{20}F_6NP$	$C_{19}H_{16}F_6NP$	$C_{25}H_{30}IrN$	$C_{27}H_{26}IrN$
Formula weight	383.31	403.30	536.70	556.69
<i>T</i> (K)	147(2)	147(2)	147(2)	147(2)
λ (Å)	1.54178	4.54179	0.71073	0.71073
Crystal system	orthorhombic	monoclinic	monoclinic	monoclinic
Space group	Pca_21	$P2_1/c$	$P2_1/n$	$P2_1/n$
<i>Unit cell dimensions</i>				
<i>a</i> (Å)	12.8020(4)	9.0234(3)	9.1676(4)	9.2735(6)
<i>b</i> (Å)	10.4478(3)	30.2757(11)	24.0869(12)	16.4837(10)
<i>c</i> (Å)	12.9417(4)	6.4577(2)	9.4239(5)	13.5643(8)
α (°)	90	90	90	90
β (°)	90	95.024(3)	100.976(1)	104.371(2)
γ (°)	90	90	90	90
<i>V</i> (Å ³)	1730.99(9)	1757.4(1)	2042.91(17)	2008.6(2)
<i>Z</i>	4	4	4	4
<i>D</i> _{calc} (Mg/m ³)	1.471	1.524	1.745	1.841
Absorption coefficient (mm ⁻¹)	1.983	1.994	6.545	6.661
<i>F</i> (000)	792	824	1056	1088
Crystal size (mm ³)	0.370 × 0.180 × 0.040	0.180 × 0.140 × 0.030	0.190 × 0.150 × 0.100	0.180 × 0.140 × 0.050
θ (°)	4.231–67.096	2.919–66.920	1.691–27.585	1.982–27.521
Index ranges	–14 ≤ <i>h</i> ≤ 15, –12 ≤ <i>k</i> ≤ 12, –15 ≤ <i>l</i> ≤ 15	–10 ≤ <i>h</i> ≤ 10, –35 ≤ <i>k</i> ≤ 35, –7 ≤ <i>l</i> ≤ 7	–11 ≤ <i>h</i> ≤ 10, –32 ≤ <i>k</i> ≤ 31, –12 ≤ <i>l</i> ≤ 12	–12 ≤ <i>h</i> ≤ 12, –21 ≤ <i>k</i> ≤ 21, –13 ≤ <i>l</i> ≤ 17
Reflections collected	39364	22960	26871	33932
Independent reflections (<i>R</i> _{int})	3067 (0.0429)	3089 (0.0662)	4720 (0.0244)	4613 (0.0522)
Completeness to $\theta = 25.00^\circ$	98.4%	98.8%	100.0%	100.0%
Absorption correction	Semi-empirical from equivalents	Semi-empirical from equivalents	Semi-empirical from equivalents	Semi-empirical from equivalents
Maximum and minimum transmission	0.7529 and 0.5962	0.7529 and 0.5962	0.7456 and 0.5760	0.7456 and 0.5112
Refinement method	Full-matrix least-squares on <i>F</i> ²	Full-matrix least-squares on <i>F</i> ²	Full-matrix least-squares on <i>F</i> ²	Full-matrix least-squares on <i>F</i> ²
Data/restraints/parameters	3067/1/232	3089/0/303	4720/0/246	4613/0/262
Goodness-of-fit (GOF) on <i>F</i> ²	1.088	1.035	1.227	1.083
Final <i>R</i> indices [<i>I</i> > 2 σ (<i>I</i>)]	<i>R</i> ₁ = 0.0293, <i>wR</i> ₂ = 0.0768	<i>R</i> ₁ = 0.0410, <i>wR</i> ₂ = 0.0872	<i>R</i> ₁ = 0.0221, <i>wR</i> ₂ = 0.0383	<i>R</i> ₁ = 0.0241, <i>wR</i> ₂ = 0.0441
<i>R</i> indices (all data)	<i>R</i> ₁ = 0.0310, <i>wR</i> ₂ = 0.0781	<i>R</i> ₁ = 0.0554, <i>wR</i> ₂ = 0.0943	<i>R</i> ₁ = 0.0291, <i>wR</i> ₂ = 0.0400	<i>R</i> ₁ = 0.0448, <i>wR</i> ₂ = 0.0513
Largest difference peak and hole (e Å ⁻³)	0.341 and –0.218	0.182 and –0.269	1.260 and –0.802	3.027 and –1.914

Selected distances (Å) and angles (°): $L^1-H_2^+ PF_6^-$: N1–C1, 1.515(3), C1–C2, 1.511(4), C2–C3, 1.545(4), N1–C1–C2, 112.61(2), C1–C2–C3, 113.18(3). $L^2-H_2^+ PF_6^-$: C16–C1, 1.377(3), C1–N1, 1.352(3), C1–C2, 1.490(3), C2–C3, 1.545(3), N1–C1–C2, 118.41(2), C1–C2–C3, 113.32(19). $L^1Ir(COD)$: (C3/C4 centroid)–Ir1, 2.026(3), (C7/C8 centroid)–Ir1, 2.128(3), C9–Ir1, 2.174(3), N1–Ir1, 2.180(3), (C3/C4 centroid)–Ir1–(C7–C8 centroid), 84.73(12), (C3/C4 centroid)–Ir1–C9, 95.01(12), (C7/C8 centroid)–Ir1–N1, 98.10(11), C9–Ir1–N1, 82.83(11), Ir1–C9–C22, 106.57(2), Ir1–N1–C23, 107.06(19). $L^2Ir(COD)$: (C3/C4 centroid)–Ir1, 2.028(4), (C7/C8 centroid)–Ir1, 2.016(4), C9–Ir1, 2.180(4), N1–Ir1, 2.099(3), (C3/C4 centroid)–Ir1–(C7–C8 centroid), 86.52(14), (C3/C4 centroid)–Ir1–C9, 98.99(14), (C7/C8 centroid)–Ir1–N1, 95.04(14), C9–Ir1–N1, 79.45(13), Ir1–C9–C22, 105.88(2), Ir1–N1–C23, 116.20(3).

is most likely caused by steric clash between N-methyls of L^1 and the COD diolefin ligand, as highlighted in the space-filling part of Fig. 2.

2.3. Reaction with hydrogen

Addition of 1 atm of hydrogen at room temperature to both complexes in benzene-*d*₆ resulted in formation of dark, iridium-containing powder, protonated ligand L^1-H/L^2-H , cyclohexane-*d*₆, and cyclooctane (as determined by ¹H NMR). This indicates that both complexes are effective hydrogenation precatalysts. The decomposition of both $L^1Ir(COD)$ and $L^2Ir(COD)$ appears to be due to hydrogenation of COD and metal reduction. Iridium nanoparticles are known to catalytically hydrogenate aromatic species [7]. Production of micro/nano-powder was observed to occur within 5 min for $L^1Ir(COD)$ and within 1 h for $L^2Ir(COD)$. We then tested for catalytic hydrogenation of neat toluene under 1 atm of H₂ at room temperature using a 0.1 molar solution of catalyst (1% catalyst loading) of $L^1Ir(COD)$ and $L^2Ir(COD)$. The reaction was monitored by ¹H NMR, and we observed slow hydrogenation of toluene (Fig. 3). The two complexes were compared to the activity of [Ir(COD)Cl]₂ under identical conditions, and both showed signif-

icantly slower rates of conversion. As can be seen from Fig. 3, this appears in part to be due to a longer induction period for $L^1Ir(COD)$ and $L^2Ir(COD)$ when compared to [Ir(COD)Cl]₂.

3. Summary and conclusion

Two new iridium complexes were obtained and structurally characterized, rare late-transition metal complexes of an N-donor-functionalized η^1 fluorenyl ligand. The complex containing a dimethylamino group, in ligand L^1 , contains a longer Ir–N bond length compared to the complex containing a pyridyl group, in ligand L^2 . Somewhat surprisingly, and likely due to steric clash, the COD also appears more weakly bonded in $L^1Ir(COD)$. Consistent with the idea that ligands are more weakly bonded in $L^1Ir(COD)$, this complex decomposes faster than $L^2Ir(COD)$ under identical hydrogenation conditions (1 atm of H₂, toluene, RT). It may be concluded that even more strongly bonded spectator ligands would be needed to keep such iridium complexes stable under hydrogenation conditions, for homogeneous hydrogenation catalysis. The two complexes do, however, serve as pre-catalysts for heterogeneous catalysis of arene hydrogenation.

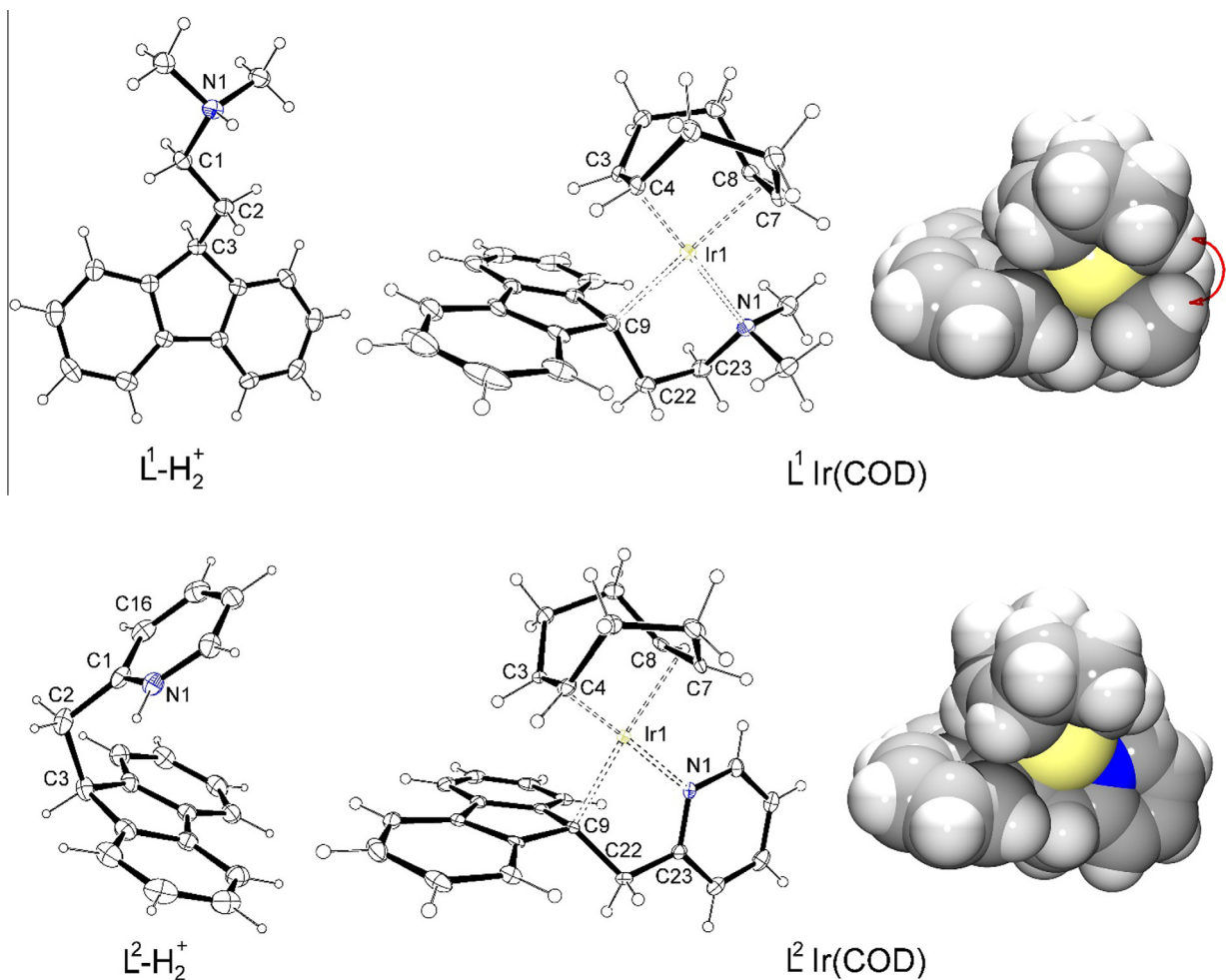


Fig. 2. Molecular structures of the cationic, protonated ligands $L^1-H_2^+$ and $L^2-H_2^+$, left (PF_6^- counterions not shown) and the metal complexes $L^1Ir(COD)$ and $L^2Ir(COD)$, middle (using 30% probability anisotropic displacement ellipsoids) and right (space-filling). The steric clash between N-methyls and COD for $L^1Ir(COD)$ is highlighted in the space-filling picture. Selected distances and angles are reported in the legend of Table 1.

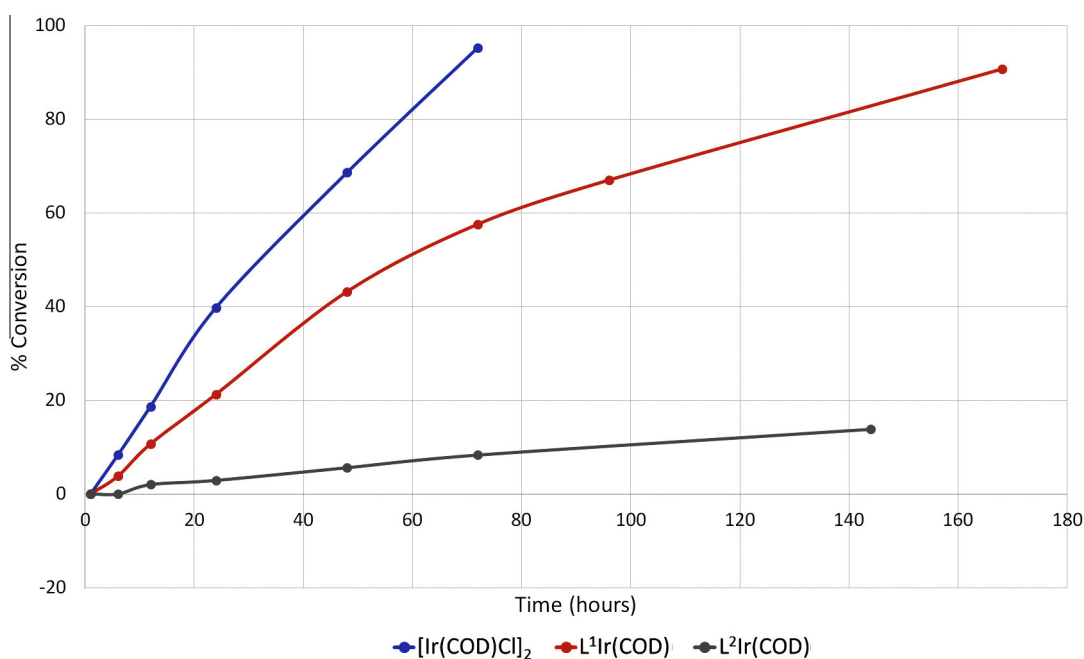


Fig. 3. Hydrogenation of toluene to methylcyclohexane as catalyzed by each of $[Ir(COD)Cl]_2$, $L^1Ir(COD)$ and $L^2Ir(COD)$ (0.1 M solution; 1% catalyst loading) at 1 atm hydrogen and room temperature. $[Ir(COD)Cl]_2$ achieved 95% conversion after 72 h, $L^1Ir(COD)$ achieved 90% conversion after 168 h and $L^2Ir(COD)$ achieved 14% conversion after 144 h.

4. Experimental

4.1. General information, reagents and precursors

Unless otherwise stated, all reagents were purchased from Sigma Aldrich and used without further purification. Solvents were degassed under vacuum and dried either on activated molecular sieves (CH_2Cl_2) or sodium benzophenone ketyl (THF, Et_2O , toluene, C_6D_6). All reactions were performed under an atmosphere of dry argon in either a glove box or using Schlenk techniques. NMR data was obtained on a Bruker Avance III 400 MHz spectrometer, all spectra were referenced to solvent residual peaks.

$\text{L}^1\text{-H}_2^+\text{PF}_6^-$: 2.0 g (13.8 mmol) of 2-chloro-N,N-dimethylethylamine hydrochloride was suspended in THF, and 9 mL (14.4 mmol) of n-butyllithium (1.6 M in hexanes) were added dropwise with stirring. The reaction was allowed to stir for 2 h at room temperature. 2.3 g of fluorene (13.8 mmol) were dissolved in THF and 9 mL (14.4 mmol) of n-butyllithium were added dropwise with stirring. The reaction was allowed to stir for ~1 h at room temperature. The fluorenyl lithium solution was added to the 2-chloro-N,N-dimethylethylamine solution and allowed to react with stirring overnight at 60 °C in a Pyrex bomb. The reaction was quenched with water and extracted with ether. The ether extract was dried with magnesium sulfate and gravity-filtered. The solvent was removed *in vacuo* and the dried product was reacted with an equivalent (13.8 mmol) of concentrated HCl in water to yield 2-(9H-fluoren-9-yl)-N,N-dimethylethylammonium chloride. The 2-(9H-fluoren-9-yl)-N,N-dimethylethylammonium chloride solution was reacted with a saturated solution containing 2.5 g (13.8 mmol) of KPF_6 in water. The product was allowed to settle out of the aqueous solution overnight, and the water layer was discarded, any residual water was removed *in vacuo*. The product was recrystallized from CH_2Cl_2 and 2.6 g (50%) of 2-(9H-fluoren-9-yl)-N,N-dimethylethylammonium hexafluorophosphate were isolated. X-ray quality crystals were obtained during the CH_2Cl_2 recrystallization.

^1H NMR (400 MHz, 298 K, D_2O ref δ 4.79): δ 7.85 (d, 2H, J = 7.4 Hz, fluorenyl); δ 7.62 (d, 2H, J = 7.3, fluorenyl); δ 7.47 (t, 2H, J = 7.5 Hz, fluorenyl); δ 7.42 (t, 2H, J = 7.4 Hz, fluorenyl); δ 4.23 (bt, 1H, J = 4.3 Hz, fluorenyl); δ 2.67 (s, 6H, CH_3); δ 2.50–2.59 (m, 4H, CH_2). Elemental analysis of $\text{C}_{17}\text{H}_{20}\text{N}^+\text{PF}_6^-$ (383.31 g/mol): Calc. C, 53.27; H, 5.26; N, 3.65; found: C, 53.94; H, 5.28; N, 3.67%.

$\text{L}^2\text{-H}_2^+\text{PF}_6^-$: 2.5 g (15.0 mmol) of fluorene were dissolved in THF, 9.35 mL (15.0 mmol) of n-butyllithium were added to the reaction dropwise with stirring. The reaction was allowed to stir for 2 h at room temperature. 1.5 g (6 mmol) of 2-(bromomethyl)pyridine hydrobromide were added to the fluorenyl lithium solution and allowed to react overnight at room temperature. Isopropanol was added to the reaction mixture and solvent was removed *in vacuo*. The resulting 2-((9H-fluoren-9-yl)methyl)pyridine was reacted with an equivalent (6 mmol) of concentrated HCl in water to yield 2-((9H-fluoren-9-yl)methyl)pyridine-1-ium chloride. The 2-((9H-fluoren-9-yl)methyl)pyridine-1-ium chloride solution was reacted with a saturated solution containing 1.1 g (6 mmol) of KPF_6 in water. The product was allowed to settle out of the aqueous solution overnight and the water layer was discarded, any residual water was removed *in vacuo*. The product was recrystallized from CH_2Cl_2 and isolated 1.6 g (66%) of 2-((9H-fluoren-9-yl)methyl)pyridine-1-ium hexafluorophosphate. X-ray quality crystals were obtained directly by recrystallization from CH_2Cl_2 .

^1H NMR (400 MHz, 298 K, CD_2Cl_2 ref δ 5.32): δ 8.41 (d, 1H, J = 6.8 Hz, pyridyl); δ 8.04 (t, 1H, J = 7.8 Hz, pyridyl); δ 7.66 (m, 3H, fluorenyl + pyridyl); δ 7.56 (d, 2H, J = 6.1 Hz, fluorenyl); δ 7.38 (m, 4H, fluorenyl); δ 7.05 (d, 1H, J = 8.1 Hz, pyridyl); δ 4.59 (t, 1H, J = 5.7 Hz, fluorenyl); δ 3.87 (d, 2H, J = 5.6 Hz, CH_2). Small

amount of THF present. Elemental analysis of $\text{C}_{19}\text{H}_{16}\text{N}^+\text{PF}_6^-$ (404.10 g/mol): Calc. C, 56.58; H, 4.00; N, 3.47; found: C, 58.10; H, 3.99; N, 3.55%.

$\text{L}^1\text{Ir}(\text{COD})$: 100 mg (0.26 mmol) of $\text{L}^1\text{-H}_2^+\text{PF}_6^-$ were suspended with 24 mg (1 mmol) NaH in THF, with 1% potassium *tert*-butoxide and allowed to react with stirring overnight at room temperature. 87 mg (0.13 mmol) of $[\text{Ir}(\text{COD})\text{Cl}]_2$ was added to the NaL^1 solution and allowed to react with stirring for 1 h. The resulting $(\text{COD})\text{Ir}(\text{L}^1)$ solution was filtered through basic alumina. The solvent was removed *in vacuo* to yield 120 mg (95%) of $\text{L}^1\text{Ir}(\text{COD})$. X-ray quality crystals were obtained from a saturated toluene solution at room temperature.

^1H NMR (400 MHz, 298 K, C_6D_6 ref δ 7.16): δ 8.01 (d, 2H, J = 7.6 Hz, fluorenyl); δ 7.48 (t, 2H, J = 7.5 Hz, fluorenyl); δ 7.44 (t, 2H, J = 7.5 Hz, fluorenyl); δ 7.28 (t, 2H, J = 7.4 Hz, fluorenyl); δ 3.00 (bs, 2H, COD CH); δ 2.54 (t, 2H, J = 6.4 Hz, L^1CH_2); δ 2.09 (s, 6H, L^1CH_3); δ 2.02 (bs, 2H, COD CH); δ 1.94 (t, 2H, J = 6.4 Hz, L^1CH_2); δ 1.87 (m, 2H, COD CH_2); δ 1.57 (m, 2H, COD CH_2); δ 1.18 (m, 2H, COD CH_2); δ 1.00 (m, 2H, COD CH_2). Elemental analysis of $\text{L}^1\text{Ir}(\text{COD})$ (532.70 g/mol): Calc. C, 56.37; H, 4.92; N, 2.63; found: C, 56.58; H, 4.00; N, 3.47%.

$\text{L}^2\text{Ir}(\text{COD})$: The synthesis of $\text{L}^2\text{Ir}(\text{COD})$ was performed similarly to $\text{L}^1\text{Ir}(\text{COD})$ and yielded 140 mg (95%) of $\text{L}^2\text{Ir}(\text{COD})$. X-ray quality crystals were obtained from a saturated toluene solution at room temperature.

^1H NMR (400 MHz, 298 K, C_6D_6 ref δ 7.16): δ 8.05 (d, 2H, J = 7.4 Hz, fluorenyl); δ 7.70 (d, 1H, J = 5.9 Hz, pyridyl); δ 7.32 (t, 2H, J = 7.2 Hz, fluorenyl); δ 7.26 (t, 2H, J = 7.2 Hz, fluorenyl); δ 6.99 (d, 2H, J = 7.6 Hz, fluorenyl); δ 6.85 (t, 1H, J = 7.9 Hz, pyridyl); δ 6.71 (d, 1H, J = 8.1 Hz, pyridyl); δ 6.28 (t, 1H, J = 6.1 Hz, pyridyl); δ 3.69 (s, 2H, L^2CH_2); δ 3.47 (bs, 2H COD CH); δ 2.57 (bs, 2H COD CH); δ 1.98 (m, 2H COD CH_2); δ 1.86 (m, 2H COD CH_2); δ 1.42 (m, 4H COD CH_2). Small amount of THF present. Elemental analysis of $\text{L}^2\text{Ir}(\text{COD})$ (552.69 g/mol): Calc. C, 58.67; H, 4.01; N, 2.53; found: C, 58.25; H, 4.71; N, 2.52%.

4.2. Reaction with hydrogen

The following procedure was performed using $\text{L}^1\text{Ir}(\text{COD})$. 51 mg (0.10 mmol) of $\text{L}^1\text{Ir}(\text{COD})$ were dissolved in 1 mL of toluene in a Pyrex bomb. The sample was exposed to a continuous flow of H_2 at room temperature and ambient pressure while stirring. NMR samples were obtained directly from the reaction mixture after 1, 6, 12, 24, 48, and 72 h. Turnover was determined by ^1H NMR through integration of the emerging methylcyclohexane peaks. ^1H NMR (400 MHz, 298 K, C_6D_6 ref δ 7.16) at 24 h: δ 7.13 (d, 2H, J = 7.3 Hz, toluene Ar-H); δ 7.02 (m, 3H, toluene Ar-H); δ 2.11 (s, 3H, toluene CH_3); δ 0.88 (d, 3H, J = 6.4 Hz, methylcyclohexane CH_3). The process was repeated under identical conditions and identical catalyst loading (1 mol%) of $\text{L}^2\text{Ir}(\text{COD})$ and $[\text{Ir}(\text{COD})\text{Cl}]_2$ (conversions shown in Fig. 3).

Acknowledgements

We thank the University of Toronto, as well as the Natural Sciences and Engineering Research Council (NSERC) of Canada, for support. A syringe grant (Hamilton Syringes) is gratefully acknowledged.

Appendix A. Supplementary data

CCDC 1404289, 1404290, 1404291, and 1404292 contains the supplementary crystallographic data for $\text{L}^1\text{Ir}(\text{COD})$, $\text{L}^2\text{Ir}(\text{COD})$, $\text{L}^1\text{-H}_2^+\text{PF}_6^-$, and $\text{L}^1\text{-H}_2^+\text{PF}_6^-$. These data can be obtained free of charge

via <http://www.ccdc.cam.ac.uk/conts/retrieving.html>, or from the Cambridge Crystallographic Data Centre, 12 Union Road, Cambridge CB2 1EZ, UK; fax: (+44) 1223-336-033; or e-mail: deposit@ccdc.cam.ac.uk.

Supplementary data associated with this article can be found, in the online version, at <http://dx.doi.org/10.1016/j.poly.2015.08.023>.

References

- [1] (a) P.J. Shapiro, E. Bunel, W.P. Schaefer, J.E. Bercaw, *Organometallics* 9 (1990) 867;
(b) W.E. Piers, P.J. Shapiro, E.E. Bunel, J.E. Bercaw, *Synlett* 2 (1990) 74;
(c) J. Okuda, *Chem. Ber.* 123 (1990) 1649;
(d) K.C. Hultsch, P. Voth, K. Beckerle, T.P. Spaniol, J. Okuda, *Organometallics* 19 (2000) 228;
(e) L.A. Williams, T.J. Marks, *Organometallics* 28 (2009) 2053;
(f) C. Wang, G. Erker, G. Kehr, K. Wedeking, R. Fröhlich, *Organometallics* 24 (2005) 4760;
(g) B.D. Stubbert, T.J. Marks, *J. Am. Chem. Soc.* 129 (2007) 4253;
(h) A. Raith, P. Altmann, M. Jokoja, W.A. Herrmann, F.E. Kühn, *Coord. Chem. Rev.* 254 (2010) 608;
(i) M. Delferro, T.J. Marks, *Chem. Rev.* 111 (2011) 2450.
- [2] J. Cano, K. Kunz, *J. Organomet. Chem.* 692 (2007) 4411.
- [3] H. Braunschweig, F.M. Breitling, *Coord. Chem. Rev.* 250 (2006) 2691.
- [4] H. Shen, Z. Xie, *Chem. Commun.* (2009) 2431.
- [5] (a) M. Tomoi, T. Yoneyama, H. Kakiuchi, *Bull. Chem. Soc. Jpn.* 48 (1975) 1285;
(b) H. Miao, S. Wang, S. Zhou, Y. Wei, Z. Zhou, H. Zhu, S. Wu, H. Wang, *Inorg. Chim. Acta* 363 (2010) 1325.
- [6] C.M. Gordon, J.D. Holbrey, A.R. Kennedy, K.R. Seddon, *J. Mater. Chem.* 8 (1998) 2627.
- [7] (a) E. Bayram, M. Zahmakiran, S. Özkaz, R.G. Finke, *Langmuir* 26 (2010) 12455;
(b) Y. Tonbul, M. Zahmakiran, S. Özkaz, *Appl. Catal. B., Environ.* 148–149 (2014) 466;
(c) V. Mévellec, A. Roucoux, E. Ramirez, K. Philippot, B. Chaudret, *Adv. Synth. Catal.* 346 (2004) 72.